

RESEARCH ARTICLE

An Isoform of Ataxin-3 Accumulates in the Nucleus of Neuronal Cells in Affected Brain Regions of SCA3 Patients

Thorsten Schmidt¹, G. Bernhard Landwehrmeyer², Ina Schmitt¹, Yvon Trottier³, Georg Auburger⁴, Franco Laccone⁵, Thomas Klockgether⁶, Michael Völpel⁷, Jörg T. Epplen¹, Ludger Schöls⁸, Olaf Riess¹

¹ Molecular Human Genetics, Ruhr-University, 44780 Bochum, Germany

² Department of Neurology, Albert-Ludwigs-University, 79106 Freiburg, Germany

³ IGBMC, CNRS, INSERM, Université Louis Pasteur, Parc d'Innovation-1, rue Laurent Fries, 67404 Illkirch Cedex, C.U. de Strasbourg, France

⁴ Division of Neurology, University Hospital, 40225 Düsseldorf, Germany

⁵ Institute for Human Genetics, University Göttingen, Goßlerstrasse 12d, 37073 Göttingen, Germany

⁶ Department of Neurology, Rheinische Friedrich-Wilhelms-Universität, 53105 Bonn, Germany

⁷ Department of Neuropathology, Klinikum Krefeld, Lutherplatz 40, 47805 Krefeld, Germany

⁸ Department of Neurology, St. Josef Hospital, Gudrunstrasse 56, 44791 Bochum, Germany

Autosomal dominant spinocerebellar ataxias (SCA) form a group of clinically and genetically heterogeneous neurodegenerative disorders. The defect responsible for SCA3/Machado-Joseph disease (MJD) has been identified as an unstable and expanded (CAG)_n trinucleotide repeat in the coding region of a novel gene of unknown function. The *MJD1* gene product, ataxin-3, exists in several isoforms. We generated polyclonal antisera against an alternate carboxy terminus of ataxin-3. This isoform, ataxin-3c, is expressed as a protein of approximately 42 kDa in normal individuals but is significantly enlarged in affected patients confirming that the CAG repeat is part of the ataxin-3c isoform and is

translated into a polyglutamine stretch, a feature common to all known CAG repeat disorders. Ataxin-3 like immunoreactivity was observed in all human brain regions and peripheral organs studied. In neuronal cells of control individuals, ataxin-3c was expressed cytoplasmatically and had a somatodendritic and axonal distribution. In SCA3 patients, however, C-terminal ataxin-3c antibodies as well as anti-ataxin-3 monoclonal antibodies (1H9) and anti-ubiquitin antibodies detected intranuclear inclusions (NIs) in neuronal cells of affected brain regions. A monoclonal antibody, 2B6, directed against an internal part of the protein, barely detected these NIs implying proteolytic cleavage of ataxin-3 prior to its transport into the nucleus. These findings provide evidence that the alternate isoform of ataxin-3 is involved in the pathogenesis of SCA3/MJD. Intranuclear protein aggregates appear as a common feature of neurodegenerative polyglutamine disorders.

Introduction

The autosomal dominantly inherited cerebellar ataxias (ADCAs) are clinically and genetically heterogeneous (36). Based on genetic linkage data at least seven gene loci are responsible for SCAs. One subtype, Machado-Joseph disease (MJD), has originally been described in families of Portuguese-Azorean origin (22, 33, 47). Clinically, variable combinations of cerebellar ataxia, pyramidal signs, dystonic-rigid extrapyramidal symptoms, peripheral neuropathy with amyotrophy and sensory loss, progressive external ophthalmoplegia, and faciolingual fasciculation have been described (32). Recently, Kawaguchi and colleagues (13) identified a (CAG)_n repeat motif in a novel gene on chromosome 14q32.1 which is expanded and unstable in MJD patients. Subsequently, CAG repeat expansions in the *MJD1* gene have been identified in patients with SCA type 3 (SCA3) who present with different clinical manifestations. In particular, faciolingual fasciculation and dystonia are rarely observed in SCA3 (37). Although there is no single clinical feature which would distinguish patients with SCA3/MJD from patients with other

Corresponding authors:

Olaf Riess, M.D., Molecular Human Genetics, Ruhr-University, D-44780 Bochum, Germany; Tel.: (+49) 234 700 3831; Fax: (+49) 234 709 4196; E-mail: olaf.riess@ruhr-uni-bochum.de

G. Bernhard Landwehrmeyer, M.D., Department of Neurology, Albert-Ludwigs-University, 79106 Freiburg, Germany; Tel.: (+49) 761 270 5236; Fax: (49) 761 270 5281

MJD1a	QQQRDLGGSSHPCEPATSSGALGSDLGKACSPFIMFATFTLYLT*
MJD1b	---G-----YELHVIFALHYSSFPPL*
MJD1c	-----DAMSEEDMLQAAVTMSLETVRNDLKTGEGK*
rsca3	----RP-YL-Y----T----G-R-NQAGNAMSEEDVLRATVTVSLETAKDSLKAERKK*

Figure 1. Amino acid sequence alignment of the C-terminus of the human MJD1 and rat rsca3 genes, respectively, demonstrating the different isoforms. The epitope used for peptide synthesis against which the antibody was generated is double underlined. Stars represent the stop codon.

ADCA's (7, 36), the pathological features of SCA3/MJD are distinct and differ from other types of ADCA's and other neurodegenerative disorders with polyglutamine expansions (6, 30, 31).

Brains of patients with SCA3/MJD exhibit macroscopically a moderate atrophy of pons and spinal cord and show shrinkage of the pallidum, subthalamic nucleus, and substantia nigra to a variable degree (42). Microscopically, neuronal loss and marked gliosis are found in a distinct set of subcortical regions including the pontine nuclei, the dentate nucleus of the cerebellum, the subthalamic nucleus, the pallidum and brainstem oculomotor nuclei (III and IV), anterior spinocerebellar tract and Clarke's column as well as a more moderate and variable degeneration in the substantia nigra, brainstem nuclei (nucl. ambiguus, V, VIII and XII), the anterior horn of the spinal cord, and anterior nerve roots (42). RNA expression studies showed that the *MJD1* gene is widely expressed in various tissues and throughout the brain in both humans and rodents (23, 35). This fact does not explain the selective, region-specific neuronal cell death observed in SCA3/MJD brains.

Several molecular biological studies provided evidence for alternate transcripts (25, 35), three of them differing in the C-terminus of the protein (8, 35, 39, 46). Two isoforms, *MJD1a* and *MJD1b*, are caused by an intragenic polymorphism, Stop361Tyr, which affects the stop codon and is in linkage disequilibrium with the (CAG)_n expansion in the Japanese or European alleles (8,40). Here we analyzed the gene product of one isoform, ataxin-3c, which is caused by alternative splicing of the *MJD1* gene and results in an alternate C-terminus comprising of 30 amino acids (8). This isoform does not have a counterpart like the stop codon polymorphism Stop361Tyr and, in contrast to the ataxin-3a carboxyl terminal domain, is predicted to be hydrophilic. We performed a detailed analysis of the ataxin-3c protein distribution in neuronal and nonneuronal human tissues of control and SCA3-affected individuals. Furthermore, we provide evidence (i) that ataxin-3 is expressed from the

normal and from the expanded allele in approximately equal amounts, (ii) that ataxin-3 is expressed cytoplasmatically in neuronal cells throughout the human brain, but (iii) that it aggregates as ubiquitinated intranuclear inclusion bodies in affected brain regions.

Materials and Methods

DNA analysis. Genomic DNA of patients with cerebellar ataxia and unaffected individuals was extracted from peripheral white blood cells (20). 100 ng genomic DNA was amplified by PCR using the primer sequences MJD52/MJD25 (13) as described (36). PCR product sizes were determined by comparison to an M13 sequencing ladder.

Antibodies. Rabbits were immunized with a peptide (NH₂-CLETVRNDLKTGEGK-COOH) directed against a C-terminal ataxin-3 isoform conjugated with keyhole limpet hemocyanin (KLH). The polyclonal antiserum was affinity purified by adsorption to the peptide (Eurogentec, Seraing, Belgium). The antiserum was diluted 1:1000 both for immunoblot analyses and for immunohistological studies. For preblockade controls, antibodies were preincubated overnight at 4°C with the peptide (1 µg/100 µl). Polyclonal antibodies to ubiquitin were purchased from DAKO (Carpinteria, CA, USA) and monoclonal ubiquitin antibodies from Biotrend (Cologne, Germany). Monoclonal antibodies 1H9 and 2B6 specifically bind ataxin-3 at regions amino-terminal to the glutamine tract (26) and will be published in more detail in a separate publication (Trottier et al., unpublished data).

Lymphoblastoid cell lines. Permanent human lymphoblastoid cell lines were established by transfecting purified human lymphoblast cells using Epstein-Barr virus. Lymphoblastoid cells from controls and SCA3/MJD-patients were cultured in DMEM medium (Seromed, Biochrom, Berlin, Germany) supplemented with antibiotics and 10% fetal calf serum.

Cell lysis. For isolation of protein, cells were washed with phosphate buffered saline, collected by centrifugation and incubated in ice-cold TNES (50 mM Tris pH 7.5; 1% Nonidet NP-40; 2 mM EDTA; 100 mM NaCl) containing a cocktail of protease inhibitors (10 mg/ml aprotinin; 0.1 M PMSF; 10 mg/ml leupeptin; 0.1 M vanadate) for 15 minutes at 4°C. Debris were removed by centrifugation.

Gel electrophoresis and immunoblot analysis. Proteins were quantified using a protein assay (Bio-Rad, Munich, Germany) according to Bradford (1) and subjected to electrophoresis on SDS-polyacrylamide (10%) gels (30 µg protein in each lane) (15). Prestained high molecular weight protein marker (Amersham, Buckinghamshire, England) was run in adjacent lines. Proteins were transferred electrophoretically to nitrocellulose membranes (Schleicher & Schuell, Dassel, Germany) (44). After transfer, blots were preincubated in 10% low fat dry milk in Tris-buffered saline (10 mM Tris pH 7.5; 150 mM NaCl) plus 0.1% Tween-20 (TBST) for 2 h at room temperature or overnight at 4°C to block non-specific sites.

After incubation with primary antibody, blots were washed four times with TBST for 15 min each. The four washing steps were repeated after incubation (1 h) with the secondary antibody (anti-rabbit antibody coupled to horseradish peroxidase, Amersham). Results were visualised using the enhanced chemiluminescence ECL-system (Amersham) and blots were exposed to Hyper-film (Amersham).

Immunofluorescence. For immunofluorescence, SK-N-AS (neuroblastoma) cells were grown on cover slips and fixed with methanol (-20°C) for 5 min. After washing with PBS, unspecific binding capacities were blocked with 10% fetal calf serum in PBS containing 0.2% Triton X-100 (30 min, 37°C). Following three washing steps in PBS, cells were incubated with the anti-ataxin-3 antibody (diluted 1:250 in PBS containing 5% normal goat serum) overnight at 4 °C in a humidified chamber. After three washes with PBS / 0.2% Triton X-100 (each for 15 min), cells were incubated with a secondary antibody conjugated with Fluorescein (Boehringer Mannheim, Mannheim, Germany) for 1 hour at 37°C. Coverslips were mounted with VectaShield (Vector) and sealed around the perimeter with nail polish.

Human tissues. Human brain tissues from 5 neurologically and neuropathologically normal donors and 4 patients from genetically verified SCA3/MJD families were included in this study. Human brain tissue from numerous brain regions, liver, spleen, kidney and heart were fixed in 10% buffered formalin, paraffin embedded and cut in 6 µm thick sections. In addition, frozen brain tissue from 2 SCA3 patients and 3 normal controls were studied.

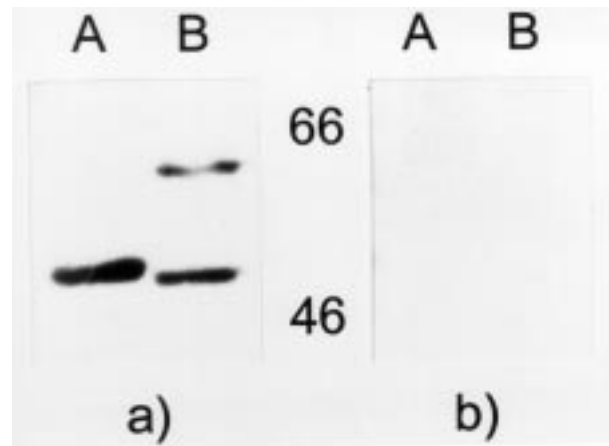


Figure 2. Western blot analysis for ataxin-3c. Wild-type ataxin-3c migrates at about 50 kDa whereas the mutant form has a higher molecular mass of approximately 60 kDa (a). Specificity of the staining is demonstrated by preincubation of the ataxin-3c antiserum with the peptide (b). A: Human neuroepithelioma cells (TC32). B: Lymphoblastoid cell line of a SCA3 patient.

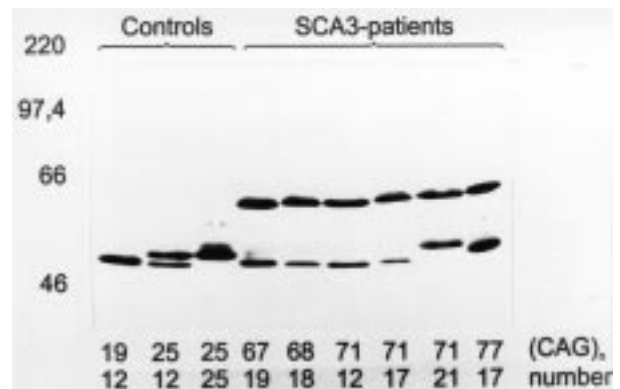


Figure 3. Western blot analysis of human lymphoblasts in control individuals and SCA3 patients. The size of the polymorphic (CAG)_n repeat is reflected by the size of the ataxin-3c protein. The length of the (CAG)_n repeats is indicated underneath each sample with the size of the normal alleles in the lower row.

Immunohistochemistry. The histological sections were stained by standard immunohistochemical techniques, with minor modifications. Briefly, following deparaffination, treatment with methanol/H₂O₂ (40% / 1% in PBS) for 10 min, and blocking (5% normal goat serum in PBS + 0.3% Triton X-100; 30 min), sections of paraffin-embedded tissue were incubated overnight or for 36 h at 4°C with anti-ataxin-3 antiserum. Antibody labeling was visualized using the Vectastain elite avidin-biotin-peroxidase complex method (Vector Laboratories, Burlingame, CA, USA) and 3,3'-diaminobenzidine (Vector) as peroxidase substrate. Sections were dehydrated through graded ethanols and xylene and viewed

Region	Density of immunoreactive neurons ¹	Intensity of ataxin3c-IR per labelled cell ¹	Subcellular distribution ²
Layer I	+	+	c
Layer II	++	+	c
Layer III	+++	+++	c
Layer IV	++	+	c
Layer V	+++	+++	c
Layer VI	+++	++	c
Hippocampus			
Dentate gyrus	+++	+	c
CA1	+++	++	c
CA2	+++	++	c
CA3	+++	++	c
CA4	+++	++	c
Striatum			
Accumbens nucleus	++	+	c
Caudate nucleus	++	+++	c
Putamen	+	++	c
Globus pallidus ext.	++	++	c
Globus pallidus int.	++	+	c+n (?)
Clastrum	+	++	c
Subthalamic nucleus	++	++	c
Thalamus	++	++	c

¹ Density of immunoreactive neurons: + few labelled cells, ++ scattered labelled cells, +++ numerous labelled cells. Intensity of ataxin-3c-IR per labelled cell: + light labelling, ++ moderate labelling, +++ dense labelling. ² c: cytoplasmic, n: nuclear

Table 1. Distribution of ataxin-3c-IR in normal human brain: telencephalon and diencephalon.

Region	Density of immunoreactive neurons ¹	Intensity of ataxin3c-IR per labelled cell ¹	Subcellular distribution ²
Substantia nigra			
Pars compacta	++	+	c
Pars reticulata	+++	++	c
Superior collicular nucleus	++	+	c
Periaqueductal gray	+++	++	c
Oculomotor nerv nucleus	+++	+++	c
Pontine nuclei	+++	+++	c
Locus coeruleus	++	+	c
Reticular formation	++	+	c
Inferior olivary nucleus	+++	+++	c
Cerebellum			
Granular layer	+	+	c
Golgi cells	++	++	c
Purkinje cells	+++	+++	c
Molecular cell layer	+++	+++	c
Dentate nucleus	+++	+++	c + n (?)
Spinal cord			
Dorsal horn	+++	++	c
Zona intermedia	+++	+++	c
Ventral horn	+++	+++	c

¹ Density of immunoreactive neurons: + few labelled cells, ++ scattered labelled cells, +++ numerous labelled cells. Intensity of ataxin-3c-IR per labelled cell: + light labelling, ++ moderate labelling, +++ dense labelling. ² c: cytoplasmic, n: nuclear

Table 2. Distribution of ataxin-3c-IR in normal brain: mes-, met- and myelencephalon and cerebellum.

using a light microscope and Nomarski optics.

Cyostat sections (20 µm) of frozen postmortem brain tissue were fixed in either 4% paraformaldehyde in PBS or 15% saturated picric acid / 4% paraformaldehyde in PBS before methanol/H₂O₂ exposure.

Results

Detection of ataxin-3 by Western blot analysis. One KLH-linked peptide representing an alternate C-terminal region of ataxin-3 (LETVRNDLKTEGKK, Fig. 1) was used for immunization of rabbits to generate polyclonal antisera. Two rabbits with low immunoreactivity against protein extract of human lymphoblasts have been used for immunisation. Antiserum obtained after three repeated immunisations still detected several unspecific bands but also the expected protein of approximately 50 kDa, respectively. Affinity purification of the polyclonal antiserum reduced the cross-reactivity to other proteins. In protein extract of lymphoblastoid cell lines from SCA3/MJD patients two bands of approximately 50 and 60 kDa were detected, representing both the normal and mutant ataxin-3 protein (Fig. 2a). Specificity of the antibodies was confirmed by preincubation of the antiserum with the peptide used for immunisation of the rabbits (Fig. 2b). Individuals carrying the expanded CAG repeat in the *MJD1* gene can clearly be distinguished by the presence of an enlarged 60 kDa immunoreactive ataxin-3c band exclusively found in affected individuals (Fig. 3). The size of the polyglutamine expansion is reflected by the apparent size of the detected protein. The generated antiserum was specific for the human ataxin-3 protein and did not detect rodent ataxin-3 in various neuronal and nonneuronal cell lines (Fig. 4).

Intracellular localization of ataxin-3 in neuronal cell lines. To assess the subcellular distribution of ataxin-3c protein, we stained human neuronal SK-N-AS cells with polyclonal antiserum against ataxin-3 (Fig. 5). Ataxin-3c is diffusely distributed in the cytoplasm and to a lesser extent in the nuclei of the cells.

Immunolocalization of ataxin-3 in normal human brain. The regional and cellular distribution of ataxin-3c immunoreactivity (ataxin-3c-IR) was studied in several regions of normal human brain including cerebral cortex, striatum, globus pallidus, thalamus, substantia nigra, cerebellum, pons, inferior olive and spinal cord. In all regions examined ataxin-3c-like IR was observed (Tables 1 and 2; Figs. 6 and 7). The most prominent

staining was associated with neuronal profiles (Figs. 6 and 7). In addition, there was some staining of glial cells (Figs. 6 and 7F). The intensity of ataxin-3c-IR varied among the neurons within each region examined. In subpopulations of neurons we observed strong IR, in others only light staining. Examples include the inhomogenous staining pattern of neurons within the cerebral cortex (Fig. 6) and in striatum where only subpopulations of neurons displayed strong staining. Neuronal staining in brain areas known to be affected in SCA3/MJD was not strikingly more intense than in regions thought to be spared from neurodegeneration. For example, intense signals were observed in Purkinje cells, a population of neurons relatively spared in SCA3/MJD (Fig. 7A). Within neurons, ataxin-3c-IR was seen preferentially in the cytoplasm, typically excluding the nucleus (Fig. 7A-E). Staining was observed in neuronal somata and extended into primary dendrites of numerous neurons (Figs. 6 and 7A). In addition, the linear fine ataxin-3c-IR in white matter tracts of cerebellar and cerebral cortex suggest that axons contain ataxin-3 as well. Consistent with an expression of ataxin-3c-IR in both dendritic and axonal neuronal processes we observed a punctate and linear staining of the neuropil in cerebral cortex, striatum, globus pallidus and cerebellum with IR of different sizes (very fine and coarse; Fig. 7G). In addition, we studied peripheral tissues including muscle, liver, heart and kidney from controls and a patient with SCA3/MJD (Fig. 7H). Staining in these organs was light and preferentially cytoplasmatic in the respective cells.

Immunolocalization of ataxin-3 in SCA3 affected brains. Immunohistochemical studies on selected areas of brains of SCA3 patients demonstrated that there was no difference in the regional and cellular distribution pattern of ataxin-3c-IR. Neuronal labelling persisted in all regions examined and demonstrated a similar variability in intensity within subpopulations of neurons as in control brain. Neuropil staining was similar to the labelling in normal brains suggesting that the somatodendritic and axonal localisation of ataxin-3c-IR persisted in brains expressing mutant ataxin-3. In affected areas like the pons neuronal loss was readily apparent. The remaining pontine neurons continued to express ataxin-3c-IR. In contrast to normal brain, however, we observed at the subcellular level small dot-like accumulations of ataxin-3c-IR in the nuclei of neurons in affected brain regions (Fig. 8A, E-G). Staining of neighbouring sections with an antibody against ubiquitin demonstrated that these intranuclear inclusions (NIs) were



Figure 4. Western blot for ataxin-3c. Ataxin-3c antiserum specifically recognizes human ataxin-3 as demonstrated for various cell lines. E: HeLa cells. F: TC32 cells. G: lymphoblastoid cell line of an affected patient. Ataxin-3 of rodents is not detected by our ataxin-3c antibody as shown for A: NS20Y cells (mouse), B: 108CC15 cells (rat/mouse hybrid), C: PC12 cells (rat), and D: CHO cells (hamster). A weak unspecific immunoreactive band with a slightly higher molecular weight of approx. 55 kDa is seen in NS20Y cells (lane A).

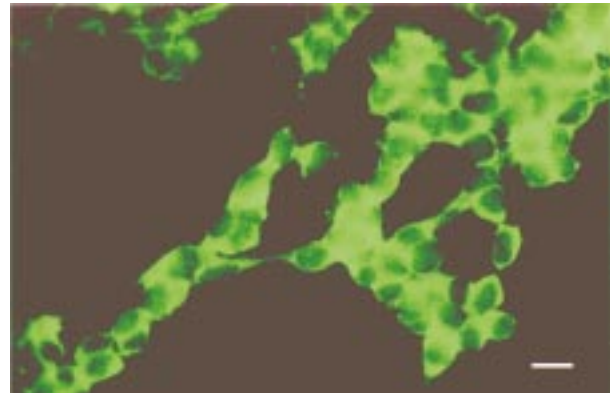


Figure 5. Ataxin-3c-IR in the neuronal cell line SK-N-AS (human neuroblastoma) demonstrating the cytoplasmatic localization of ataxin-3c by immunofluorescence. Bar = 20 μ m.

ubiquitin-positive (Fig. 8B). Immunohistochemistry with the monoclonal antibody 1H9 resulted in an intense labelling of neuronal NIs (Fig. 8C). Typically, NIs visualized with the monoclonal antibody 1H9 appeared intensely stained. In contrast, staining with the antibody 2B6 which recognizes a more aminoterminal epitope of ataxin-3 resulted in no (or an occasional very faint) staining of intranuclear inclusions (Fig. 8D) although this antibody clearly detects normal cytoplasmic distribution of the protein. A monoclonal antibody against the reaction product of transglutaminase, N-epsilon-(gamma-glutamyl)-lysine, did not stain NIs (not shown). Intranuclear deposits of ataxin-3-IR were visible in numerous (but not all) neurons of the affected regions. In most instances there was one inclusion per

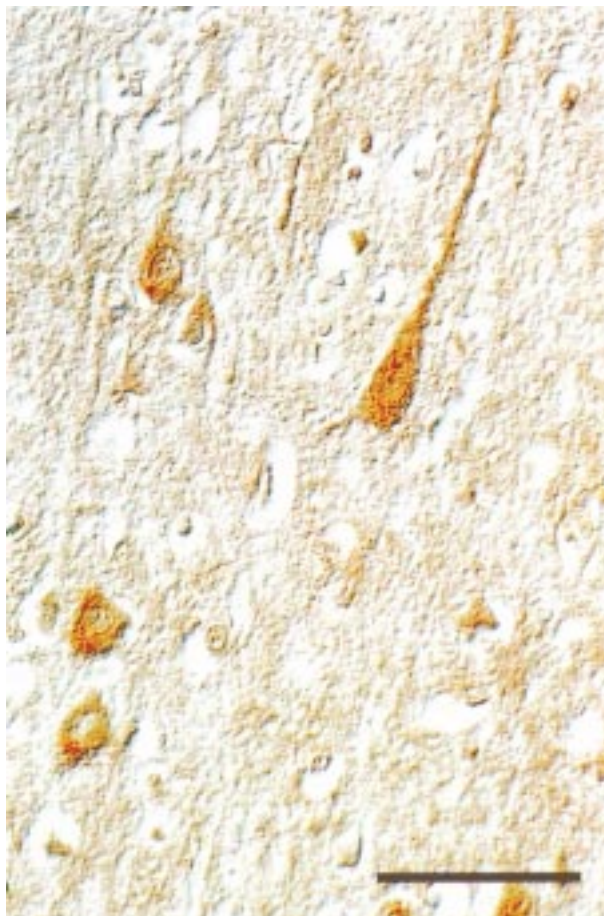


Figure 6. Immunohistochemistry using the ataxin-3c-antibody in normal human postmortem frontal cortex demonstrates a predominantly neuronal pattern of immunostaining. Neurons are stained with various intensity resulting in an inhomogeneous pattern. In neurons, immunostaining was preferentially associated with somatodendritic domains (see the intensely stained primary dendrite of the large neuron to the right). In addition, some small cellular profiles were immunostained presumably representing glial cells. Bar = 100 μ m. Nomarski-optics.

nucleus; occasionally we observed two or three inclusion bodies per nucleus. However, NIs were not observed in regions unaffected by the disease like cerebral or cerebellar cortex.

Discussion

SCA3/MJD is a neurodegenerative disorder with onset in midlife caused by the expansion of an unstable (CAG)_n repeat in a novel gene of unknown function. A growing list of neurodegenerative disorders including SCA1 (24), SCA2 (12), SCA6 (29, 49), SCA7 (3), spinobulbar muscular atrophy (SBMA) (17), Huntington's disease (HD) (43) and dentatorubral pallidolusian atro-

phy (DRPLA) (14, 21) is caused by this dynamic mutation in unrelated genes. In the present study we analyzed an isoform of the MJD1 gene product, ataxin-3c, carrying an alternate C-terminus. The physiological function of ataxin-3 is still unknown; there are no structural domains or significant homologies to proteins of known function to assign a physiological role to ataxin-3. Consequently, the functional relevance of the alternate C-terminus is unclear.

Immunoblotting and immunohistochemistry showed that ataxin-3c is expressed in nonneuronal and neuronal tissues. In normal human brain, ataxin-3c-like IR exhibited predominantly neuronal expression in all brain regions studied. At the cellular level, we observed a preferentially cytoplasmic localisation of ataxin-3c in neuronal cell lines and post-mortem human brain. These findings agree well with observations reported by Paulson et al. who used a polyclonal fusion protein antibody directed against the entire protein (harboring an internal 45-bp deletion) which did not distinguish between the different C-terminal isoforms (25). The good match in the distribution of ataxin-3 observed with these two antibodies (and with the monoclonal antibodies 1H9 and 2B6; data not shown) suggests that the ataxin-3c isoform is present in most (if not all) ataxin-3 expressing cells in human brain.

For SCA3/MJD, the pattern of neuronal loss differs from other ADCA's and other neurodegenerative disorders with polyglutamine expansions (6, 30, 31). Clinical features have been linked to a selective neuronal loss in distinct brain areas and a consequent degeneration of fibre tracts (6, 33, 42). For example, ataxia in SCA3/MJD is thought to result from degeneration of cerebellar afferents and efferents including neurons in vestibular and pontine nuclei, the spinocerebellar tract, the cerebellar peduncle and the dentate nucleus, respectively. Unlike in SCA1, SCA2 and SCA6 there is no marked degeneration of Purkinje cells or of the cerebellar cortex. Lid retraction and external ophthalmoplegia, commonly observed in patients with SCA3/MJD, is thought to be related to cell loss in the periaqueductal grey and in the oculomotor and trochlear nerve nuclei. Amyotrophy may be due to loss of cranial motor nerve cells and anterior horn cells in spinal cord and rigid and dystonic features (particularly prominent in patients with early onset of symptoms) to neuronal loss in substantia nigra pars compacta, subthalamic nucleus and globus pallidus. We observed ataxin-3c-IR in all neuronal populations affected in SCA3/MJD (Tables 1 and 2). In addition, however, ataxin-3c IR was present in numerous brain regions like the cerebral and the cere-

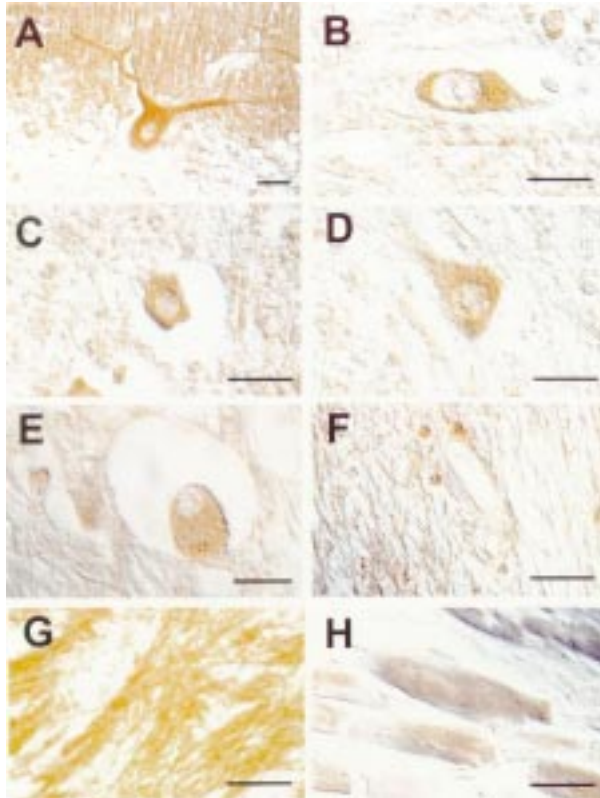


Figure 7. Ataxin-3c immunoreactivity in normal human tissues. Immunoreactivity of individual neurons in various brain regions demonstrating a preferentially cytoplasmatic distribution of ataxin-3c-immunoreactivity. **A:** Cerebellum: Purkinje cell layer. **B:** Pons. **C:** Striatum. **D:** Globus pallidus. **E:** Inferior olive. **F:** Ataxin-3c immunoreactivity was also seen in some cellular profiles with a glial morphology, e.g. in globus pallidus. **G:** An intense immunoreactivity associated with neurites was particularly striking in globus pallidus. The morphology of the immunoreactive neurites is consistent with the presence of ataxin-3c in both dendrites and axons. **H:** Ataxin-3c immunoreactivity in heart muscle cells. Bars = 20 μ m. Nomarski-optics.

bellar cortex, the striatum and the olivary nuclei where no obvious neuronal loss or gliosis has been reported in symptomatic patients (2, 6, 32, 42). Interestingly, the intensity of ataxin-3c IR varied between neurons suggesting that ataxin-3c is more abundant in some neuronal populations than in others. However, there was no obvious relationship between the apparent intensity of the IR and the likelihood of neurons to undergo degeneration. A striking example is the intense IR observed in Purkinje cells known to be comparatively little affected by the disease process. Therefore, as in other polyglutamine diseases, the expression of the *MJD1* gene itself is not sufficient to explain the restricted and distinct neuropathology characteristic for SCA3/MJD.

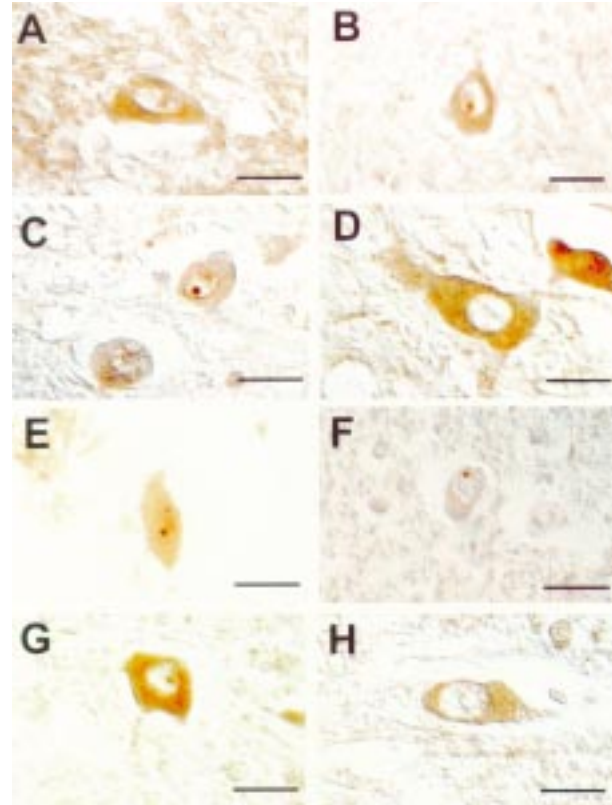


Figure 8. Ataxin-3c-IR in neurons from SCA3 brains. **A:** Pons: NIs immunoreactive to the ataxin-3c-antibodies. **B:** Pons: NIs immunoreactive to ubiquitin. **C:** Pons: NIs immunoreactive to the monoclonal antibody 1H9 directed against a region of ataxin-3 proximal to the polyglutamine chain. **D:** Pons: Absence of immunoreactivity of NIs using the monoclonal antibody 2B6 which is directed against a more N-terminal region of ataxin-3. **E:** Pons: Several NIs immunoreactive to the polyclonal antibody ataxin-3c. **F:** Spinal cord: NI body immunoreactive to the ataxin-3c antibody. **G:** Pons: NI immunoreactive to the ataxin-3c antibody. **H:** For comparison, the preferentially cytoplasmatic ataxin-3c IR in pontine neurons of normal controls. Bars = 20 μ m. Nomarski-optics

The mechanism underlying neuronal cell death in polyglutamine diseases is unknown. There is substantial evidence from histopathological studies that the $(CAG)_n$ expansion does not alter the expression patterns and levels in any of the affected genes (16, 23). In all disorders with $(CAG)_n$ expansions including the recently discovered SCA6 (TS and OR, unpublished observation), the $(CAG)_n$ repeats are part of the predicted coding region and have been shown to be translated into elongated polyglutamine tracts. Our ataxin-3c antisera confirms that in the ataxin-3c isoform the polymorphic $(CAG)_n$ repeat is indeed translated into an elongated polyglutamine stretch in SCA3/MJD patients supporting earlier

evidence using a monoclonal antibody, 1C2, directed against elongated Gln_{>40} motifs (45). We also demonstrate that ataxin-3c is expressed from the normal and the expanded allele in approximately equal amounts.

The polyglutamine expansion in the mutant ataxin-3c alters the physical properties of ataxin-3, disproportionately delaying its migration on SDS-PAGE gels (this study; 25). The altered properties of the mutant ataxin-3 are reflected in postmortem brain: exclusively in affected brain areas we observed a subcellular redistribution of ataxin-3c in the form of intranuclear deposits. These nuclear inclusions were similar in morphology and distribution to the ones described by Paulson *et al.* (26) and have also been found in affected brain areas of HD, DRPLA, and SCA1 (4, 5, 38) as well as in transgenic models for SCA1 and HD (4, 38). Here we provide evidence that the alternate C-terminus of ataxin-3 is part of the nuclear deposits. In addition, we confirm that the monoclonal antibody 1H9 stains NIs by recognizing an epitope close to the expanded polyglutamine stretch (26). In contrast, antibodies (2B6) directed against a more N-terminal part of ataxin-3 did not or just barely stain NIs, raising the possibility that the expanded protein might be proteolytically processed prior to nuclear accumulation. Proteolytic processing prior to a nuclear aggregation is suggested by immunohistochemical findings in HD where NIs can be detected with antibodies directed against the polyglutamine containing N-terminus of huntingtin but not with antibodies against more carboxyterminal sequences (5).

There are several mechanisms by which proteins containing an expanded stretch of polyglutamines may form aggregates. Perutz has suggested that long stretches of polyglutamines may form hydrogen bonds to other extended stretches of polyglutamines in an antiparallel fashion ('polar zippers', 28) forming an aggregation of the protein in a noncovalent fashion (34, 41). Alternatively, polyglutamine stretches may aggregate following covalent linkage by transglutaminases (9). Our attempts using a monoclonal antibody to detect a reaction product of transglutaminases, N-epsilon-(gamma-glutamyl)-lysine, showed no staining of NIs under the conditions used and suggest that NIs do not result from covalent linkage due to the enzymatic activity of transglutaminases.

Aside from ataxin-3, NIs in SCA3/MJD brains contain further immunoreactive proteins like ubiquitin as has been described in HD, DRPLA, and SCA1 (4, 5, 38). Protein ubiquitination leads to protein degradation (reviewed in 10), and represents a widely used regulatory mechanism to maintain or recover the physiological

cellular environment and to reach a high turn-over for many short-lived eukaryotic proteins. Although ubiquitination is a common feature of many pathological inclusions such as the Lewy body of Parkinson's disease, it has not yet been linked to neuronal cell death. Interestingly, in neurons containing NIs we observed cytoplasmic staining with anti-ubiquitin antibodies in excess of what is usually observed in cytoplasm. The significance of this cytoplasmic staining (Fig. 8b) is uncertain but raises the possibility that this ubiquitin-IR reflects ubiquitinated, diffusely distributed cytoplasmic aggregates which might be impossible to detect by ataxin-3-antibodies since the physiological cytoplasmic ataxin-3-IR may obscure their presence. However, we did not observe distinct deposits in the cytoplasm as we did in the nucleus. NIs are detectable in the brains of transgenic models for HD (4) and SCA1 (38) before behavioral phenotypes develop but not in nonneuronal tissues of affected persons nor in brain areas spared of the neurodegenerative process. It appears therefore that NIs are a marker for neurodegeneration in CAG/glutamine expansion disorders. It is unclear at present whether these aggregates themselves are toxic to neurons or whether the expanded polyglutamine ataxin-3 causes an ataxin-3-specific disruption of neuronal function of which the formation of aggregates is a by-product. The distinctive pattern of cell loss characteristic for each polyglutamine disorder suggests that this specificity is determined by the protein context in which the extended polyglutamine segment is presented to the cell. There is some evidence from studies in SCA1 that region-specific expression of interacting proteins might influence the distinctive pattern of cell loss (18). However, so far proteins interacting with ataxin-3 selectively expressed in vulnerable brain areas have not been identified.

The human ataxin-3c antibody does not detect the rodent homologue as the epitope differs from the corresponding rat region in 6 amino acid residues. Therefore this antibody will be helpful to define characteristic pathological findings in transgenic animals expressing a human SCA3/MJD transgene. It will be interesting to learn whether transgenic animals generated with constructs harboring different C-terminal regions generate a phenotype and if so, whether the symptoms differ between the transgenic lines.

Acknowledgements

We would like to thank our colleagues of the Clinic of Neurology and the Department of Human Molecular Genetics for their support, in particular B. Lind for

expert technical assistance and C. Plehn for photography. Y.T. acknowledges the continuous support of J.L. Mandel. This study would not have been possible without the help of the SCA families which is gratefully acknowledged. Work in the lab of O.R. was supported by the BMBF and G.B.L. was supported by SFB 505. Y.T. was supported by a fellowship from the Hereditary Disease Foundation (USA). This article contains parts of the Ph.D. thesis of T.S.

References

- Bradford A (1976) A rapid and sensitive method for the quantitation of microgram quantities of protein utilizing the principle of protein-dye binding. *Analyt Biochem* 72: 248-54
- Burt T, Blumbergs P, Currie B (1993) A dominant hereditary ataxia resembling Machado-Joseph disease in Arnhem Land, Australia. *Neurology* 43: 1750-2
- David G, Abbas N, Stevanin G, Durr A, Yvert G, Cancel G, Weber C, Imbert G, Saudou F, Antoniou E, Drabkin H, Gemmill R, Giunti P, Benomar A, Wood N, Ruberg M, Agid Y, Mandel JL, Brice A (1997) Cloning of the SCA7 gene reveals a highly unstable CAG repeat expansion. *Nat Genet* 17: 65-70
- Davies SW, Turmaine M, Cozens BA, DiFiglia M, Sharp AH, Ross CA, Scherzinger E, Wanker EE, Mangiarini L, Bates GP (1997) Formation of neuronal intranuclear inclusions underlies the neurological dysfunction in mice transgenic for the HD mutation. *Cell* 90: 537-48
- DiFiglia M, Sapp E, Chase KO, Davies SW, Bates GP, Vonsattel JP, Aronin N (1997) Aggregation of huntingtin in neuronal intranuclear inclusions and dystrophic neurites in brain. *Science* 277: 1990-3
- Dürr A, Stevanin G, Cancel G, Duyckaerts C, Abbas N, Didierjean O, Chneiweiss H, Benomar A, Lyon CO, Julien J, Serdaru M, Penet C, Agid Y, Brice A (1996) Spinocerebellar ataxia 3 and Machado-Joseph disease: clinical, molecular, and neuropathological features. *Ann Neurol* 39: 490-9
- Giunti P, Sweeney M G, Harding A E (1995) Detection of the Machado-Joseph disease/spinocerebellar ataxia three trinucleotide repeat expansion in families with autosomal dominant motor disorders, including the Drew family of Walworth. *Brain* 118: 1077-85
- Goto J, Watanabe M, Ichikawa Y, Yee S B, Ihara N, Endo K, Igarashi S, Takiyama Y, Gaspar C, Maciel P, Tsuji S, Rouleau GA, Kanazawa I (1997) Machado-joseph-disease gene products carrying different carboxyl termini. *Neurosci Res* 28: 373-7
- Green H (1993) Human genetic diseases due to codon reiteration: relationship to an evolutionary mechanism. *Cell* 74: 955-6
- Hochstrasser M (1996) Ubiquitin-dependent protein degradation. *Annu Rev Genet* 30: 405-39
- Ikeda H, Yamaguchi M, Sugai S, Aze Y, Narumiya S, Kakizuka A (1996) Expanded polyglutamine in the Machado-Joseph disease protein induces cell death in vitro and in vivo. *Nat Genet* 13: 196-202
- Imbert G, Saudou F, Yvert G, Devys D, Trottier Y, Garnier JM, Weber C, Mandel JL, Cancel G, Abbas N, Durr A, Didierjean O, Stevanin G, Agid Y, Brice A (1996) Cloning of the gene for spinocerebellar ataxia 2 reveals a locus with high sensitivity to expanded cag/glutamine repeats. *Nat Genet* 14: 285-91
- Kawaguchi Y, Okamoto T, Taniwaki M, Aizawa M, Inoue M, Katayama S, Kawakami H, Nakamura S, Nishimura M, Akiguchi I, Kimura J, Naru-miya S, Kakizuka A (1994) CAG expansions in a novel gene for Machado-Joseph disease at chromosome 14q32.1. *Nat Genet* 8: 221-8
- Koide R, Ikeuchi T, Onodera O, Tanaka H, Igarashi S, Endo K, Takahashi H, Kondo R, Ishikawa A, Hayashi T, Saito M, Tomoda A, Miike T, Naito H, Ikuta F, Tsuji S (1994) Unstable expansion of CAG repeat in hereditary dentatorubral-pallidoluysonian atrophy (DRPLA). *Nat Genet* 6: 9-13
- Laemmli, UK (1970) Cleavage of structural proteins during assembly of the head of bacteriophage T4. *Nature* 227: 680-5
- Landwehrmeyer GB, McNeil SM, Dure LS, Ge P, Aizawa H, Huang Q, Ambrose CM, Duyao MP, Bird ED, Bonilla E, DeYoung M, Avila-Gonzales AJ, Wexler NS, DiFiglia M, Gusella JF, MacDonald ME, Penney JB, Young AB, Vonsattel JP (1995) Huntington's disease gene: regional and cellular expression in brain of normal and affected individuals. *Ann Neurol* 37: 218-30
- LaSpada AR, Wilson EM, Lubahn DB, Harding AE, Fischbeck H (1991) Androgen receptor gene mutations in X-linked spinal and bulbar muscular atrophy. *Nature* 352: 77-9
- Matilla A, Koshy BT, Cummings C, Isobe T, Orr HT, Zoghbi HY (1997) The cerebellar leucine-rich acidic nuclear protein interacts with ataxin-1. *Nature* 389: 974-8
- Matsumura R, Takayanagi T, Fujimoto Y, Murata K, Mano Y, Horikawa H, Chuma T (1996) The relationship between trinucleotide repeat length and phenotypic variation in Machado-Joseph disease. *J Neurol Sci* 139: 52-7
- Miller SA, Dykes DD, Polesky HF (1988) A simple salting out procedure for extracting DNA from human nucleated cells. *Nucleic Acids Res* 16: 1215
- Nagafuchi S, Yanagisawa H, Sato K, Shirayama T, Ohsaki E, Bundo M, Takeda T, Tadokoro K, Kondo I, Murayama N, Tanaka Y, Kikushima H, Umino K, Kurosawa H, Furukawa T, Nihei K, Inoue T, Sano A, Komure O, Takahashi M, Yoshizawa T, Kanazawa I, Yamada M (1994) Dentatorubral and pallidoluysonian atrophy expansion of an unstable CAG trinucleotide on chromosome 12p. *Nat Genet* 6: 14-8
- Nakano KK, Dawson DM, Spence A (1972) Machado disease: a hereditary ataxia in Portuguese immigrants to Massachusetts. *Neurology* 22: 49-55
- Nishiyama K, Murayama S, Goto J, Watanabe M, Hashida H, Katayama S, Nomura Y, Nakamura S, Kanazawa I (1996) Regional and cellular expression of the Machado-Joseph disease gene in brains of normal and affected individuals. *Ann Neurol* 40: 776-81

24. Orr HT, Chung MY, Banfi S, Kwiatkowski TJ, Servadio A, Beaudet AL, McCall AE, Duvick LA, Ranum LP, Zoghbi HY (1993) Expansion of an unstable trinucleotide CAG repeat in spinocerebellar ataxia type 1. *Nat Genet* 4: 221-6
25. Paulson HL, Das SS, Crino PB, Perez MK, Patel SC, Gotsdiner D, Fischbeck KH, Pittman RN (1997) Machado-Joseph disease gene product is a cytoplasmic protein widely expressed in brain. *Ann Neurol* 41: 453-62
26. Paulson HL, Perez MK, Trottier Y, Trojanowski JQ, Subramony SH, Das SS, Vig P, Mandel JL, Fischbeck KH, Pittman RN (1997) Intracellular inclusions of expanded polyglutamine protein in spinocerebellar ataxia type 3. *Neuron* 19: 333-44
27. Penney JB, Vonsattel JP, Macdonald ME, Gusella JF, Myers RH (1997) Cag repeat number governs the development rate of pathology in huntingtons-disease. *Annals of Neurology* 41: 689-92
28. Perutz MF, Johnson T, Suzuki M, Finch JT (1994) Glutamine Repeats As Polar Zippers - Their Possible Role in Inherited Neurodegenerative Diseases. *Proc Natl Acad Sci USA* 91: 5355-58
29. Riess O, Schöls L, Bottger H, Nolte D, Vieira SA, Schimming C, Kreuz F, Macek MJ, Krebsova A, Macek MS, Klockgether T, Zuhlke C, Laccione FA (1997) SCA6 is caused by moderate CAG expansion in the alpha1A-voltage-dependent calcium channel gene. *Hum Mol Genet* 6: 1289-93
30. Robitaille Y, Lopescendes I, Becher M, Rouleau G, Clark AW (1997) The neuropathology of CAG repeat diseases - review and update of genetic and molecular features. *Brain Pathology* 7: 901-26
31. Robitaille Y, Schut L, Kish SJ (1995) Structural and immunocytochemical features of olivopontocerebellar atrophy caused by the spinocerebellar ataxia type 1 (SCA-1) mutation define a unique phenotype. *Acta Neuropathol (Berl)* 90: 572-81
32. Rosenberg RN (1992) Machado-Joseph disease: an autosomal dominant motor system degeneration. *Mov Disord* 7: 193-203
33. Rosenberg RN, Nyhan WL, Bay C (1976) Autosomal dominant striatonigral degeneration: a clinical, pathologic, and biochemical study of a new genetic disorder. *Neurology* 26: 703-14
34. Scherzinger E, Lurz R, Turmaine M, Mangiarini L, Hollenbach B, Hasenbank R, Bates GP, Davies SW, Lehrach H, Wanker EE (1997) Huntingtin-encoded polyglutamine expansions form amyloid-like protein aggregates in vitro and in vivo. *Cell* 90: 549-58
35. Schmitt I, Brattig T, Gossen M, Riess O (1997) Characterization of the rat spinocerebellar ataxia type 3 gene. *Neurogenetics* 1: 103-12
36. Schöls L, Vieira-Saecker A.M.M, Schöls S, Przuntek H, Epplen J.T, Riess O (1995) Trinucleotide expansion within the MJD1 gene presents clinically as spinocerebellar ataxia and occurs most frequently in German SCA patients. *Hum Mol Genet* 4: 1001-5
37. Schöls L, Amoiridis G, Buttner T, Przuntek H, Epplen JT, Riess O (1997) Autosomal dominant cerebellar ataxia - phenotypic differences in genetically defined subtypes. *Ann Neurol* 42: 924-32
37. Schöls L, Amoiridis G, Epplen JT, Langkafel M, Przuntek H, Riess O (1996) Relations between genotype and phenotype in German patients with the Machado-Joseph disease mutation. *J Neurol Neurosurg Psychiatry* 61: 466-70
38. Skinner PJ, Koshy BT, Cummings CJ, Klement IA, Helin K, Servadio A, Zoghbi HY, Orr HT (1997) Ataxin-1 with an expanded glutamine tract alters nuclear matrix-associated structures. *Nature* 389: 971-74
39. Stevanin G, Le GE, Ravise N, Chneiweiss H, Durr A, Cancel G, Vignal A, Boch AL, Ruberg M, Penet C, Pothin Y, Lagroua I, Haguenaou M, Rancurel G, Weissenbach J, Agid Y, Brice A (1994) A third locus for autosomal dominant cerebellar ataxia type I maps to chromosome 14q24.3-qter: evidence for the existence of a fourth locus. *Am J Hum Genet* 54: 11-20
40. Stevanin G, Lebre AS, Mathieux C, Cancel G, Abbas N, Didierjean O, Durr A, Trottier Y, Agid Y, Brice A (1997) Linkage disequilibrium between the spinocerebellar ataxia 3/Machado-Joseph disease mutation and two intragenic polymorphisms, one of which, X359Y, affects the stop codon. *Am J Hum Genet* 60: 1548-52
41. Stott K, Blackburn JM, Butler PJ, Perutz M (1995) Incorporation of glutamine repeats makes protein oligomerize: implications for neurodegenerative diseases. *Proc Natl Acad Sci USA* 92: 6509-13
42. Takiyama Y, Oyanagi S, Kawashima S, Sakamoto H, Saito K, Yoshida M, Tsuji S, Mizuno Y, Nishizawa M (1994) A clinical and pathologic study of a large Japanese family with Machado-Joseph disease tightly linked to the DNA markers on chromosome 14q. *Neurology* 44: 1302-8
43. The Huntington's Disease Collaborative Research Group (1993) A novel gene containing a trinucleotide repeat that is expanded and unstable on Huntington's disease chromosomes. *Cell* 72: 971-83
44. Towbin H, Staehelin T, Gordon J (1979) Electrophoretic transfer of proteins from polyacrylamide gels to nitrocellulose sheets: Procedure and some applications. *Proc Natl Acad Sci USA* 76: 4350-54
45. Trottier Y, Lutz Y, Stevanin G, Imbert G, Devys D, Cancel G, Saudou F, Weber C, David G, Tora L, Agid Y, Brice A, Mandel JL (1995) Polyglutamine expansion as a pathological epitope in Huntington's disease and four dominant cerebellar ataxias. *Nature* 378: 403-6
46. Wang G, Ide K, Nukina N, Goto J, Ichikawa Y, Uchida K, Sakamoto T, Kanazawa I (1997) Machado-Joseph disease gene product identified in lymphocytes and brain. *Biochem Biophys Res Commun* 233: 476-79
47. Woods BI, Schaumburg HH (1972) Nigro-spino-dentatal degeneration with nuclear ophthalmoplegia: a unique and partially treatable clinicopathological entity. *J Neurol Sci* 17: 149-66

48. Zhou YX, Takiyama Y, Igarashi S, Li YF, Zhou BY, Gui DC, Endo K, Tanaka H, Chen ZH, Zhou LS, Fan MZ, Yang BX, Weissenbach J, Wang GX, Tsuji S (1997) Machado-Joseph disease in four chinese pedigrees - molecular analysis of 15 patients including two juvenile cases and clinical correlations. *Neurology* 48: 482-85
49. Zhuchenko O, Bailey J, Bonnen P, Ashizawa T, Stockton DW, Amos C, Dobyns WB, Subramony SH, Zoghbi HY, Lee CC (1997) Autosomal dominant cerebellar ataxia (SCA6) associated with small polyglutamine expansions in the alpha 1A-voltage-dependent calcium channel. *Nat Genet* 15: 62-9